OPTICAL REVIEW Vol. 12, No. 4 (2005) 293–300

Color Correction of Pathological Images Based on Dye Amount Quantification

Tokiya ABE[1], Yuri MURAKAMI[2,3], Masahiro YAMAGUCHI[1,3], Nagaaki OHYAMA[2,3] and Yukako YAGI[4]

[1]*Imaging Science and Engineering Laboratory, Tokyo Institute of Technology, 4259 Nagatuta, Midori-ku, Yokohama 226-8503, Japan*
[2]*Frontier Collaborative Research Center, Tokyo Institute of Technology, 4259 Nagatuta, Midori-ku, Yokohama 226-8503, Japan*
[3]*Akasaka Natural Vision Research Center, Telecommunications Advancement Organization of Japan, 1-8-6 Akasaka, Minato-ku, Tokyo 107-0052, Japan*
[4]*University of Pittsburgh Medical Center Pittsburgh, 5230, Centre Avenue, Pittsburgh, PA 15232-1381, U.S.A.*

(Received November 2, 2004; Accepted April 21, 2005)

Pathological images are color images of stained tissue slides, the color of which varies depending on staining conditions. For reliable diagnosis, the color variation must be corrected in these images. This paper proposes a color correction method for hematoxylin and eosin (H&E) stained pathological images in which the amounts of H&E dyes are estimated based on multispectral imaging technique and Beer Lambert law, and the color image is generated corresponding to the adjusted amount of dyes. This enables us to correct an image to an arbitrary or specified optimal staining-condition image. Through experiments using H&E stained human liver slide images, the effectiveness of the proposed method was confirmed.

Key words: microscopy, pathology, spectral imaging, color reproduction, color correction

1. Introduction

In pathological diagnosis, pathologists examine the microscopic patterns in tissue slides to determine how cell and tissue morphology has changed, on which is based the final diagnosis and the subsequent treatment policy. Tissue sections are stained to enhance their contrast because original tissue sections are almost colorless; hematoxylin and eosin (H&E) stain is commonly used for routine diagnostic procedures. Since most staining reactions involve a chemical union between dye and the stained substance, the color of stained tissue sections could be determined by conditions such as the staining time, the temperature or pH of the solution.[1,2] However, it is difficult to keep the staining conditions constant in practice. Moreover, different staining-condition standards are often used depending on facilities or the pathologist. In addition, if the pathological image is captured by a digital camera, the color of the image is also affected by the characteristics of the microscope and the imaging device. As a result, the color of pathological images acquired using different time or facilities varies greatly depending on circumstances. Such color variation becomes a problem especially in telepathology,[3] in which pathological images acquired by various facilities should be examined. Therefore, in order to reach a reliable diagnosis, a color correction method is strongly required. It has been reported that color variation depending on the characteristics of input devices can be corrected by implementing color management technologies;[4–7] we also utilized these technologies in this paper. For color variation depending on staining condition, however, there has been no effective color correction method. Thus, this paper focuses on a method of correcting color variation resulting from staining conditions. Most slides including H&E stained slides are stained by multiple dyes and are prepared using multiple staining procedures. In the color correction for pathological images, the correction must be performed corresponding to each staining procedure independently.

Recently, multispectral microscopic systems have been implemented to acquire the spectral transmittance and developed for the image analysis for diagnosis support.[8–17] There are a number of spectral imaging technologies: acousto-optic tunable filters,[8] liquid crystal tunable filters,[9] Fourier transformed interferometry,[10] and variable interference filter.[17] Moreover, it has been reported that spectral information obtained from multispectral images makes it possible to estimate the amount of dyes bound to tissue in multiply stained slides.[16,17] Utilizing this technology, this paper proposes a color correction method for pathological images in which the estimated amount of dye is directly corrected and the corresponding color images are generated. This method realizes a color correction of a target image into an arbitrary staining-condition image and also into a specified optimal staining-condition image.

The proposed method is applied to H&E stained human liver slides, and the colorimetric accuracy of the corrected images is evaluated from pathological diagnostic viewpoints using a multispectral image captured by a microscopic multispectral camera with a 16-band rotating filter wheel.

2. Color Correction Method

This paper focuses on H&E stained slides. Unstained tissue slides are almost completely transparent and only red blood cells have some pigment. Therefore, after the H&E staining procedure, there are mainly three kinds of pigments in the slides: H, E and that of red blood cells. In H&E staining, H stains the nuclear region blue to purple and E stains the cytoplasm, connective tissues etc. pink to red.

2.1 Color reproduction from spectral transmittance

First, let us start with the relation between a multispectral image pixel value and the spectral transmittance of a stained slide. With the assumption that the image acquisition system has a linear optoelectronic transfer function the camera response g_k for an image pixel at kth band can be expressed as follows:

$$g_k = \int S_k(\lambda)E(\lambda)t(\lambda)\,d\lambda + n_k, \tag{1}$$

where $S_k(\lambda)$ is the spectral product of camera sensitivity and transmittance of the optical filter at kth band; $E(\lambda)$ represents the radiance of the light source. Likewise, $t(\lambda)$ is the spectral transmittance of a point in the slide and n_k is the additive noise *e.g.* random shot noise. If we measure $S_k(\lambda)$ and $E(\lambda)$ in advance, $t(\lambda)$ can be estimated from the observed g_k by means of the Wiener estimation algorithm.[16] Through these procedures, we can obtain the accurate spectral transmittance of the pixels in the slide image from its multispectral image, which is independent of both illumination and imaging device characteristics.

A colorimetric image is obtained by color imaging equation as

$$x'_j = \int M_j(\lambda)E(\lambda)t(\lambda)\,d\lambda, \tag{2}$$

where x'_j is one of the tristimulus values corresponding to color matching function $M_j(\lambda)$, such as CIE 1931 XYZ. The image for display can be generated from the tristimulus image by taking into account the characteristics of the display device.

2.2 Quantification of the amount of dye

In this section, we briefly review the quantification method of the amount of dye in a stained slide. To reveal the quantitative relation between the spectral transmittance and the dye concentration of a stained slide, the Beer Lambert law[16–18] is applied. If this law can be applied, we have

$$-\log\left\{\frac{t(\lambda)}{t_g(\lambda)}\right\} = \int_0^d \sum_{i=1}^{n} \varepsilon_i(\lambda)c_i(z)\,dz = \sum_{i=1}^{n} \varepsilon_i(\lambda)C_i, \tag{3}$$

where $t(\lambda)$ is the Wiener estimated spectral transmittance and $t_g(\lambda)$ is the spectral transmittance of the glass slide itself, which is determined experimentally; d denotes the optical path length in the slide while i represents the dye, i.e., H, E and blood cells; $\varepsilon_i(\lambda)$ and $c_i(z)$ represents the spectral absorption coefficient and the concentration distribution of the ith dye along the optical path; and C_i is the amount of the dye within the optical path. We estimate the amount of the dye C_i by means of the least squares error method, namely, minimizing

$$\int \left(-\log\left\{\frac{t(\lambda)}{t_g(\lambda)}\right\} - \sum_{i=1}^{n} \varepsilon_i(\lambda)\hat{C}_i\right)^2 d\lambda, \tag{4}$$

where $\hat{C}_i$ is the estimated amount of ith dye. Below, we use C_i instead of $\hat{C}_i$ for simplicity.

2.3 Color correction based on the amount of dye

This section explains the proposed color correction method based on the amount of dye which is estimated through the method mentioned in the previous section. H and E are contained in the stained slide, with the amount of each dye either increasing or decreasing depending on staining condition such as the staining time and temperature of solution. To correct the color variation caused by the variation of staining conditions, we make a simple modification to eq. (3): a weighting coefficient w_i is introduced to the equation:

$$-\log\left\{\frac{t'(\lambda)}{t_g(\lambda)}\right\} = \sum_{i=1}^{n=3} w_i\varepsilon_i(\lambda)C_i, \tag{5}$$

where $t'(\lambda)$ represents the corrected transmittance at an image pixel, and it is determined after the weighing factor w_i is multiplied by C_i. With the corrected transmittance obtained from eq. (5), the corrected color image of the stained slide is reproduced by eq. (2). In this method, by correcting the weighting coefficient, it is possible to generate the color image when correcting the amount of each dye independently and create the color image under an arbitrary staining condition.

2.4 Determination of weighting coefficients

Let us consider a slide with good staining condition and having the ideal color, we call this slide the 'ideal slide'. If the color of a slide is converted to the color of the ideal slide using eq. (5), the color variation due to an inappropriate staining condition can be corrected. For this purpose, the weighting coefficients w_i in eq. (5) have to be determined such that the relation

$$w_iC_i(\mathbf{r}) = C^{\mathrm{opt}}{}_i(\mathbf{r}) \tag{6}$$

is satisfied. In eq. (6) $C^{\mathrm{opt}}{}_i(\mathbf{r})$ denotes the amount of the i-th dye in the ideal slide. To determine w_i independent of either $\mathbf{r}$ or C_i, we recall a following chemical kinetic equation. Here, one of the dyes is considered for simplicity and the subscript i is omitted in the equations below. When the concentration of the dye solution c_s is far larger than the tissue concentration $c_t(\mathbf{r})$, the amount of dye that binds to the tissue $C(\mathbf{r}, t)$ is approximately represented by

$$C(\mathbf{r}, t) \cong (1 - \exp(-\alpha_{\mathbf{r}}c_s t))c_t(\mathbf{r})d, \tag{7}$$

where $\mathbf{r}$ is the position of the slide, t is the reaction time, $\alpha_{\mathbf{r}}$ and d represent the reaction rate constant and tissue thickness, respectively. While $c_t(\mathbf{r})$ is determined by the tissue characteristics, $c_s t$ varies depending on the staining conditions. Let t^{opt} and t denote the staining time of an ideal slide and the slide actually obtained respectively, then $C(\mathbf{r})$ and $C^{\mathrm{opt}}(\mathbf{r})$ in eq. (6) can be given by

$$\begin{aligned} C(\mathbf{r}) &\cong (1 - \exp(-\alpha_{\mathbf{r}}c_s t))c_t(\mathbf{r})d \\ C^{\mathrm{opt}}(\mathbf{r}) &\cong (1 - \exp(-\alpha_{\mathbf{r}}c_s t^{\mathrm{opt}}))c_t(\mathbf{r})d \end{aligned} \tag{8}$$

If $\alpha_{\mathbf{r}}$ is constant, $C^{\mathrm{opt}}(\mathbf{r})/C(\mathbf{r})$ does not depend on $\mathbf{r}$. Therefore, w can be estimated by

$$w = \frac{C^{\mathrm{opt}}(\mathbf{r})}{C(\mathbf{r})} \tag{9}$$

The dependence of α upon $\mathbf{r}$ is discussed in the next section. Since we do not have an ideal slide we used a 'reference slide', which is stained under an optimal staining condition and with the same tissue characteristics but of a different tissue section. We also use the term 'test slide' for the slides with abnormal staining conditions, *e.g.*, over-stained and under-stained. If it is possible to select certain areas from both reference and test slide where the tissue characteristics

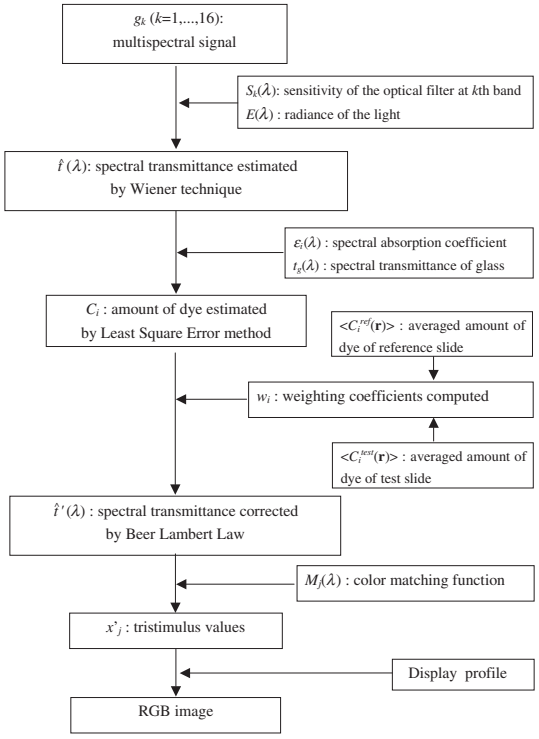

Fig. 1. Color correction method based on amount of dye.

of both areas are almost the same, we can approximately estimate w of eq. (9) by

$$\hat{w} = \frac{\langle C^{\mathrm{ref}}(\mathbf{r})\rangle}{\langle C^{\mathrm{test}}(\mathbf{r})\rangle} \tag{10}$$

where $C^{\mathrm{ref}}(\mathbf{r})$ and $C^{\mathrm{test}}(\mathbf{r})$ are the dye amounts of reference and test slides, and $\langle\cdots\rangle$ represents the average over the selected area. Equation (10) is rewritten using eq. (7) as

$$\hat{w} = \frac{\langle C^{\mathrm{ref}}(\mathbf{r})\rangle}{\langle C^{\mathrm{test}}(\mathbf{r})\rangle} = \frac{(1-\exp(-\alpha c_s t^{\mathrm{ref}}))\langle c_t^{\mathrm{ref}}(\mathbf{r})\rangle}{(1-\exp(-\alpha c_s t^{\mathrm{test}}))\langle c_t^{\mathrm{test}}(\mathbf{r})\rangle}. \tag{11}$$

where the superscripts 'ref' and 'test' are parameters that represent the reference and test slides. If the averaged areas are selected such that $\langle c_t^{\mathrm{ref}}(\mathbf{r})\rangle = \langle c_t^{\mathrm{test}}(\mathbf{r})\rangle$, it is expected that w can be estimated properly using eq. (11). In the experiments, we used a number of cytoplasm regions which are relatively spatially uniform and then used eq. (10) to calculate $\hat{w}$. An automatic selection method of the desired region is a subject for future work.

The process of the proposed color correction technique from §2.1 to 2.4 is illustrated in Fig. 1. If it is possible to select the areas with almost the same characteristics, $\langle c_t^{\mathrm{ref}}(\mathbf{r})\rangle$ can be used commonly for all slides. Only the calculation of $\langle C_i^{\mathrm{test}}(\mathbf{r})\rangle$ for the new test slide is needed. Since only the amounts of H and E are corrected, the weighing factor for red cells is set at 1.0.

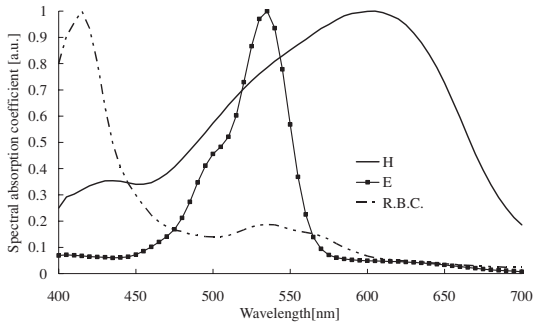

Fig. 2. Normalized spectral absorption coefficients of hematoxylin, eosin and red blood cells.

3. Experiments

3.1 Experimental conditions

In this experiment, the imaging system which was utilized to capture the multi-spectral images is composed of 2000 × 2000 pixels for the CCD camera, 16 band rotation filters, a conventional optical microscope Olympus BX-62 with an objective lens of 20 fold where the light source is a halogen lamp, and a PC based image capturing and displaying unit.[15] Wiener estimation of the spectral transmittance requires the covariance matrix of this transmittance. The covariance matrix employed in the estimation process is generated with a first-order Markov model.[19] In order to estimate the spectral transmittance accurately, a thin diffusing (white) glass-slide with approximately 95% transmittance across the 400- to 1000-nm spectral range is used as a calibration slide.

To obtain the absorption coefficients of H, E and red blood cell, $\varepsilon_i(\lambda)$, we prepared three slides, a slide stained by H only, one stained by E only and one unstained, and the optical densities of these slides were measured using a microscopic spectrophotometer (MCPD-3000). Since it is difficult to obtain the absolute spectral absorption coefficients, the normalized optical densities, shown in Fig. 2, were used as spectral absorption coefficient instead.

In this experiment, five slides of H&E stained human liver specimens were prepared under different staining conditions: normal, over-, under-, excess H, and excess E. Over- and under-stained slides were prepared with longer and shorter staining time, respectively, for both H and E stains. The slide of excess H is intensively over-stained with H, while stained normally with E. The specimens on the slides are continuous sections of one tissue, have the same thickness of about 3 μm and are stained at normal temperature of color images of these slides are shown in Fig. 3.

Since it is important to separate the nucleus area from the cytoplasm area for pathological diagnosis, the degree of the separation between nucleus and cytoplasm can be one of the measures of the staining condition. To evaluate the degree of separation of these areas from in the H&E slide, we examined the color difference between them in the CIE-LAB color space. This color difference is defined by

$$\Delta E^*_{NC} = \sqrt{(\langle L^*(N)\rangle - \langle L^*(C)\rangle)^2 + (\langle a^*(N)\rangle - \langle a^*(C)\rangle)^2 + (\langle b^*(N)\rangle - \langle b^*(C)\rangle)^2}, \tag{12}$$

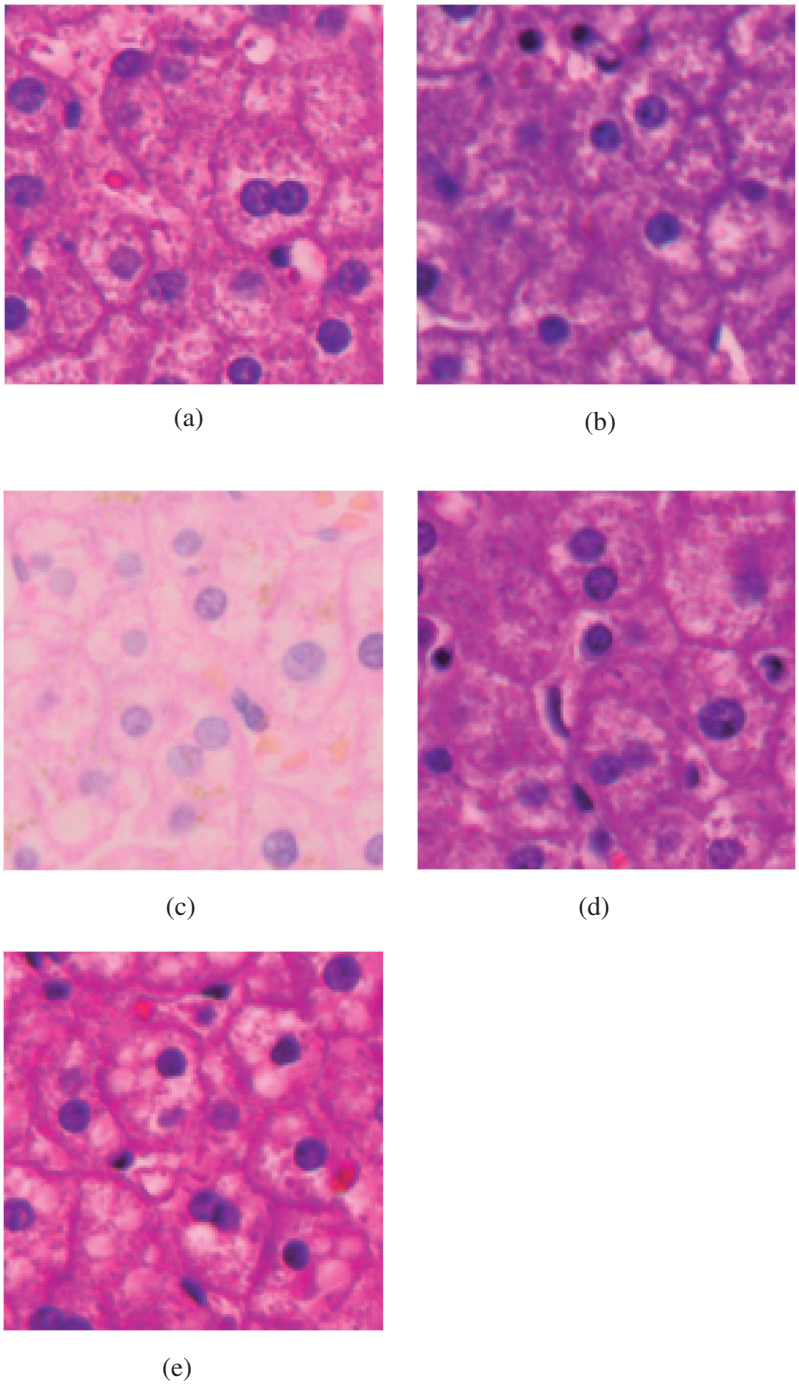

Fig. 3. Color images of stained slides: (a) normal; (b) over; (c) under; (d) excess H; (e) excess E. These images are generated from the multispectral image of the tissue.

where $(L^*(N), a^*(N), b^*(N))$ and $(L^*(C), a^*(C), b^*(C))$ represent CIE-LAB values in the nucleus area and the cytoplasm area, respectively. The color difference between the two areas, ΔE^*_{NC} is used in the evaluation of the results below.

3.2 *Reaction rate constancy*

In eq. (8) we assumed that the reaction rate constant α does not depend on the location, since the tissue components of nucleus and cytoplasm are different, however, this assumption may not be valid. In the first experiment, we verify this assumption. From eq. (7) the chemical kinetic equations can be written as

$$\begin{aligned} C_N(t) &\cong \{1 - \exp(-\alpha_{\mathrm{n}} c_{\mathrm{s}} t)\} c_{\mathrm{n}} d \\ C_C(t) &\cong \{1 - \exp(-\alpha_{\mathrm{c}} c_{\mathrm{s}} t)\} c_{\mathrm{c}} d, \end{aligned} \tag{13}$$

where α_{n} and α_{c} are the reaction rates of nucleus area and cytoplasm area; c_{n} and c_{c} are the tissue concentrations in these areas, respectively, and $C_N(t)$ and $C_C(t)$ are the amount of dye in the respective areas. If $\alpha_{\mathrm{n}} = \alpha_{\mathrm{c}}$, $C_N(t)$ must be proportional to $C_C(t)$, namely, $C_N(t) = (c_{\mathrm{n}}/c_{\mathrm{c}}) C_C(t)$, for any t, then, we plot $C_N(t)$ vs $C_C(t)$ using the images of different t to check the reaction rate constancy. For this purpose we

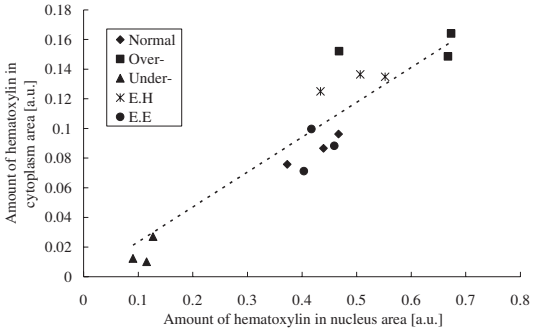

(a)

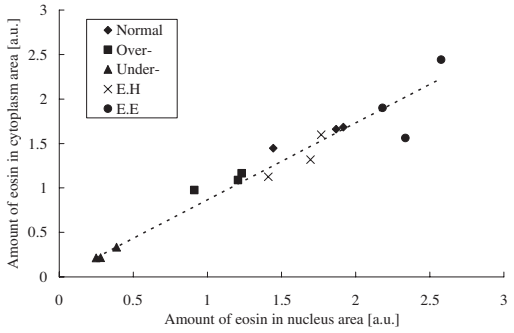

(b)

Fig. 4. The relation of the amount of (a) hematoxylin and (b) eosin between nucleus area and cytoplasm area; dotted lines are linear regression plots.

used the five slides prepared with different staining time, as explained in the previous subsection. We captured three images from different locations of each slide wherein 30 regions were selected from nucleus and cytoplasm areas and the estimated amount of dye is the averaged in each region. The average amount of dye in nucleus area and cytoplasm region, $C_N(t)$ and $C_C(t)$, is plotted as shown in Fig. 4. Each plot in (a) and (b) is calculated from one image, which corresponds to a certain staining time. The dotted line is calculated by a regression analysis. The relation between the amount of H&E dyes in nucleus and cytoplasm regions can be considered as linear as shown in (a) and (b). As a result, the constant ratio of $C_N(t)$ and $C_C(t)$ in all slides prepared for different staining times provides that the reaction rates of nucleus area and cytoplasm area are almost identical and eq. (9) is satisfied. It should be noted that the variation from the dotted line in (a) and (b) may be caused by the manual selection of nucleus and cytoplasm regions, although further investigation is needed for these substances in other tissues such as heart, kidney, etc. The color correction method proposed in this paper is confirmed to be valid through this experiment.

Figure 5 shows the estimated spectral transmittance of nucleus, cytoplasm and red blood cell. Nucleus strongly absorb at about 540 and 610 nm. As shown in Fig. 2, the spectral absorption coefficient of E and H has a peak value at this wavelength, so we can say that nucleus is stained by H and E. Figure 5 shows that the cytoplasm and red blood cells are stained by E.

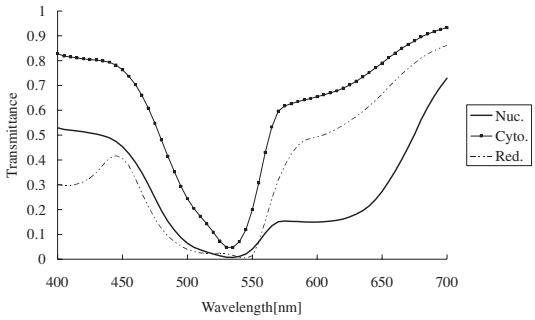

Fig. 5. The spectral transmittance estimated from multispectral signal of nucleus, cytoplasm and red blood cell.

Figure 6 shows the estimated amount of each dye for a normal H&E slide on a 200 × 200-pixel area. Figure 6(a) is the color image generated from a multispectral image based on eqs. (1) and (2) and (b)–(d) are the three decomposition images corresponding to the amount of red blood cell, H and E, respectively; the grey-level of each pixel corresponds to the amount of each dye: black to zero and white to the maximum. In Fig. 6(a), purple circular regions correspond to nucleus, small darker pink regions correspond to red blood cells, and the remaining lighter pink regions correspond to cytoplasm. We can see that white regions correspond to red blood cell areas in Fig. 6(b); the H stains mainly the nucleus area in Fig. 6(c); and the E stains the nucleus, the cytoplasm and red blood cell regions in Fig. 6(d). These results agree well with the pathological assessment, although decomposition images have a small error at the edge such as between the nucleus area and the background. This error is believed to be caused by the misalignment of the multispectral image.

3.3 Modification of dye amount

Figure 7 shows the results when changing the weighting coefficient in eq. (5) of the normal H&E slide image for the same region as in Fig. 6. The center image of Fig. 7 is the unchanged slide image, namely, $w_i = 1.0$ for both H and E. It is slightly different from Fig. 6(a) because the least squares error in eq. (4) is not zero, but the error is small and almost negligible. In Fig. 7, horizontal and vertical axes correspond to the weighting coefficients of H and E, respectively; these are varied at three levels: 0.1, 1 and 3.0 for H and E. We set the weighting coefficients of red blood cells at 1.0 for all images because the amount of red blood cell is not affected by staining condition. It can be seen that the greater the amount of H, the deeper is the violet-blue color of the image. Also, increasing the amount of E, the pink color of the image becomes deeper. As a result, it is confirmed that the amount of each dye can be contributed by eq. (5) independently in the H&E slide.

3.4 Color correction

Next, we show the results of color correction using the weighting coefficient proposed in §2.3, where the normal H&E slide is the reference slide and the under-stained H&E slide is the test slide. The weighting coefficients were calculated from cytoplasm areas where 20 points were

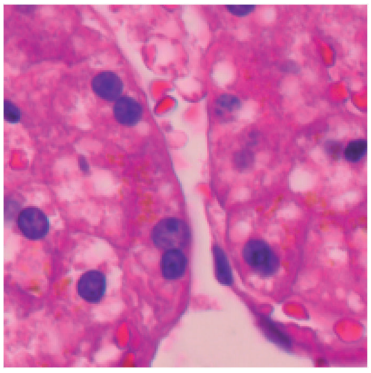

(a)

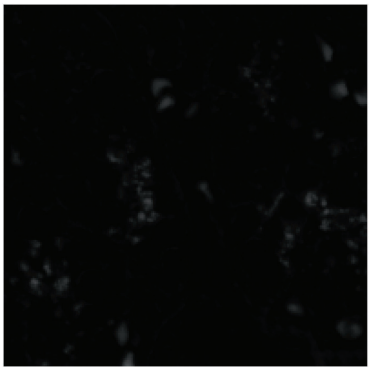

(b)

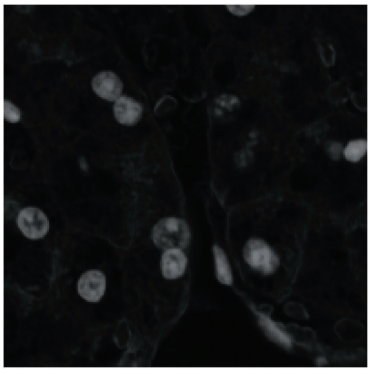

(c)

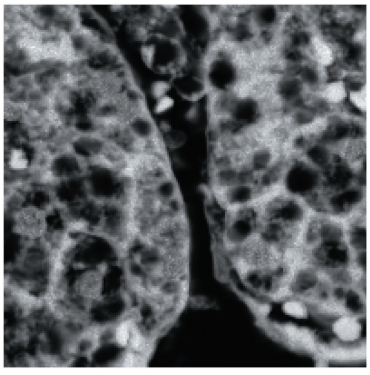

(d)

Fig. 6. Images generated from the multispectral image of a human liver tissue: (a) color image of the tissue; the multispectral image is decomposed into images corresponding to the amount of: (b) red blood cell, (c) hematoxylin, and (d) eosin.

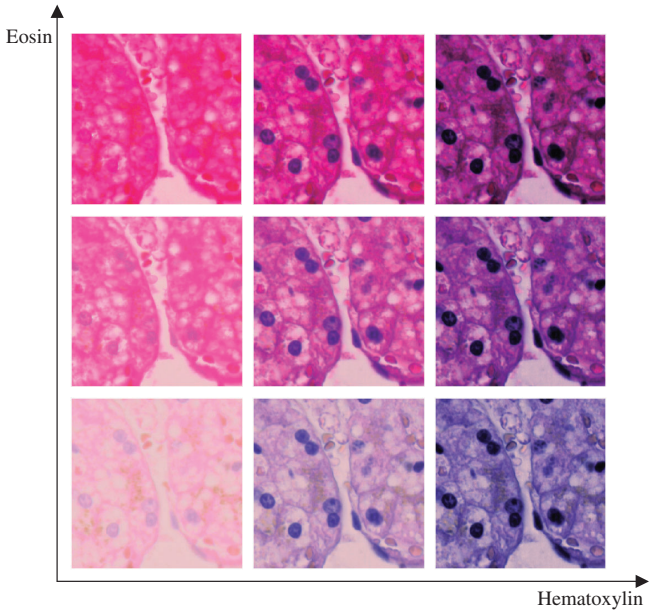

Fig. 7. The color images reproduced by adjusting the amount of hematoxylin and eosin. *X* and *Y* axes represent the weighing coefficients for hematoxylin and eosin dyes.

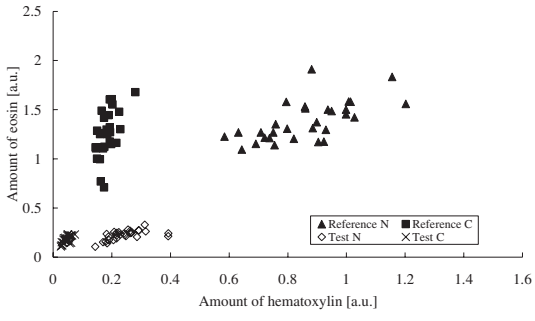

(a)

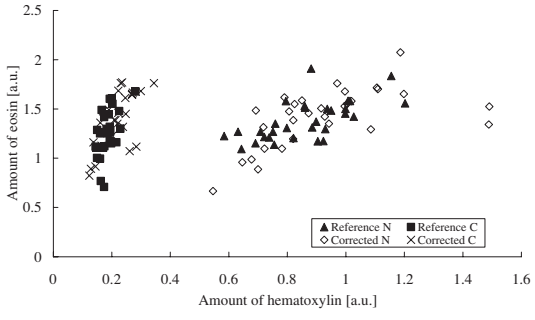

(b)

Fig. 8. (a) and (b) show the distribution of the hematoxylin and eosin amount in nucleus area and cytoplasm area in the test (understained slide) image and the corrected test image, respectively. The distribution of each dye amount in the reference image is the same for both cases, i.e., uncorrected and corrected image. In the corrected image, the distribution of H and E is closely similar to the reference slide image.

selected manually from the reference slide and the test slide. The weighting coefficients of H and E were 4.62 and 7.65, respectively; that of red blood cell is set at 1.0. The test slide

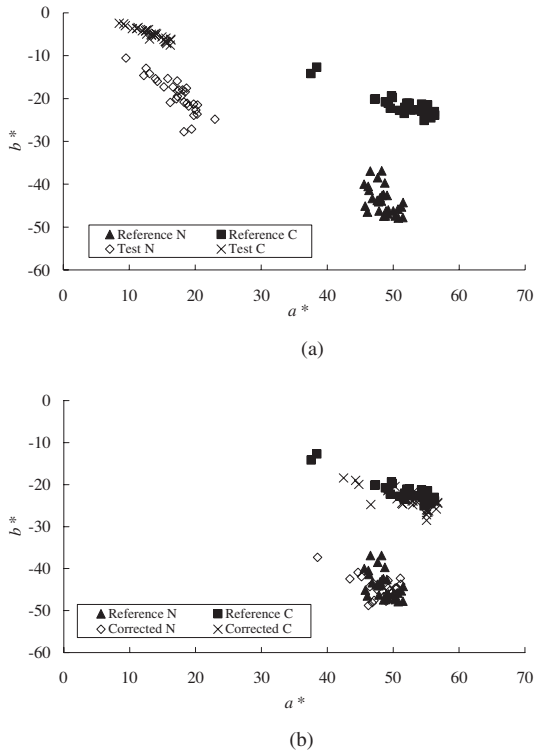

Fig. 9. The color distribution of nucleus and cytoplasm areas in a^*b^* space in the: (a) test (under stained slide) image and (b) corrected test image. As seen, the color distribution of the corrected image is almost similar to that of the reference image.

image was corrected based on these weighting coefficients.

Figure 8(a) shows the distribution of the amount of H and E in nucleus and cytoplasm areas in the test and reference slide images, while 8(b) shows the distribution of the corrected test slide image. Figure 8(a) indicates that the dye amounts of nucleus and cytoplasm areas in the test slide image are smaller than the reference slide image. On the other hand, through the color correction using the above weighting coefficient, the distribution in the corrected test slide image is almost the same as the reference slide image as shown in Fig. 8(b).

Figure 9(a) shows the color distribution of nucleus and cytoplasm areas in the test slide image with those in the reference slide image in CIE-LAB space with 30 points plotted for each region, (b) shows the color distribution of the corrected test slide image with the reference slide image. Figure 9(a) indicates that the color saturation of the test slide image is low compared to that of the reference slide image, which makes it difficult to distinguish the nucleus and the cytoplasm because there is little color difference between the two areas is minimal. It can be seen in Fig. 9(b) that the color distribution of the nucleus area and cytoplasm area in the corrected test slide image is closely similar to that in the reference slide image.

In addition, Fig. 10 shows the ΔE^*_{NC} between the nucleus and the cytoplasm for each image. The fact that the ΔE^*_{NC} value in the corrected test slide image is as high as the reference slide image implies that identification of the nucleus and the cytoplasm in the former image has improved

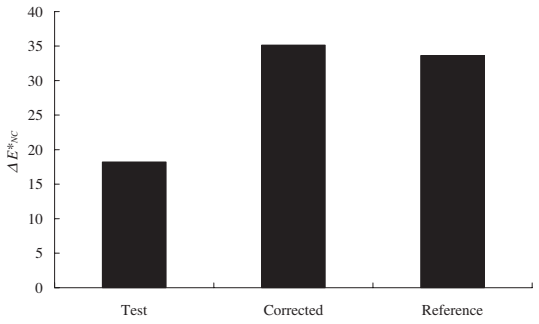

Fig. 10. ΔE^*_{NC} between the nucleus and the cytoplasm in reference, test and corrected test images.

compared with the latter.

In Figs. 8–10, the distribution of corrected test slide is slightly different from those of the reference, especially the error in the nucleus area is larger than in the cytoplasm area. In the experiment, we assumed that reaction rate constant α is independent from the area in eq. (6), and the weighting coefficients were derived based only on α of the cytoplasm area to reduce the manual operation. We can observe a small variation from the regression line in Fig. 4 and this means that the reaction rate of nucleus area slightly differs from that of the cytoplasm area. Thus the shape of the color distributions of nucleus area in the corrected test slide image slightly differs from the reference slide image. Apparently in the manual selection process it is difficult to find a spatially uniform cytoplasm area, and this causes the variation of the dye concentration in the reference slide. The improvement of correction accuracy and the automatic area selection are the subjects for future investigation.

Figure 9 shows the resultant images of color correction. To compare the test slide with the reference slide which is the normal slide, the regions having similar tissue structures were extracted from each image. Figure 9 is the corrected test slide image by the proposed method, and it can be seen that the color tone of the corrected test slide image is quite similar to the reference slide image.

4. Conclusion

We have proposed a color correction method for H&E stained pathological images in which a test image is corrected to the stained image under an arbitrary or specified staining condition. To realize this, the method utilizes the amount of dyes estimated from a multispectral image and the Beer–Lambert law. Through the experiment using an H&E stained liver slide, we confirmed that the proposed method can generate arbitrary staining-condition images. In addition, we showed that the weighting coefficient derived from the chemical kinetic equation works appropriately to correct an under-stain of test image to an ideal condition. This paper has not investigated the effect of the thickness variation of tissue slides on the amount of dye. Though we used 16 band images in this proposed method, we could further reduce the number of multispectral images if accurate statistical information of spectral transmittance were obtained in

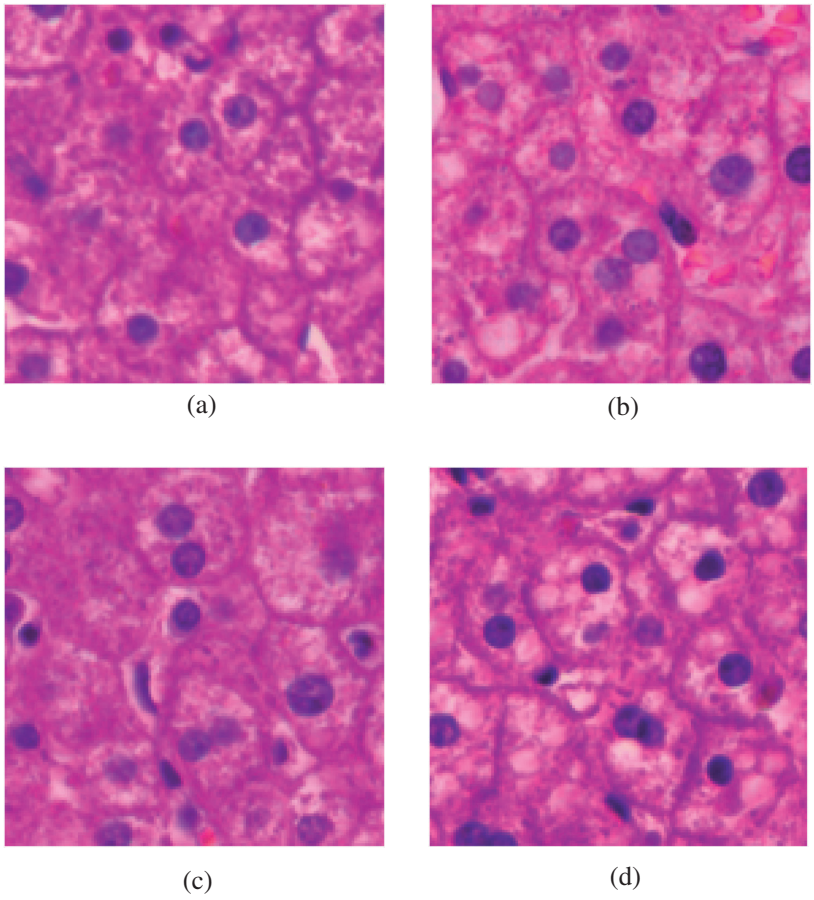

Fig. 11. Color corrected images of stained slides: (a) over-; (b) under-; (c) excess H; (d) excess E. The corrected image is generated from the images corresponding to the amount of red blood cell, H and E.

advance. In future work, we will study this using a number of slides and also adapt this method for other organs.

Acknowledgment

The authors wish to thank Mr. Yoshifumi Kanno of NTT Data Corp., Mr. Yasuhiro Komiya of Olympus Corp., and Mr. Hiroyuki Fukuda of the Akasaka Natural Vision Research Center, Telecommunications Advancement Organization (currently National Institute of Information and Communications Technology) for participating in the experiments and the discussions.

References

1) Ch. Bettinger and H. W. Zimmermann: Histochemistry **96** (1991) 215.
2) A. Gschwendtner and T. Mairinger: Anal. Cell. Pathol. **9** (1995) 29.
3) Y. Yagi, N. Azumi, A. Elsayed and S. K. Mun: Proc. SPIE **3031** (1997) 810.
4) The International Electrotechnical Commission, IEC 61966-2-1, 1999.
5) The International Color Consortium, Specification ICC.1, 2003.
6) La Commission Internationale de L'Éclairage, Publication CIE 159, 2004.
7) H. Fukuda, Y. Murakami, T. Abe, M. Yamaguchi, H. Haneishi, N. Ohyama and Y. Yagi: APIII, Pittsburgh, PA, 2003 http://apiii.upmc.edu/abstracts/posterarchive/2003/abs_include.cfm?file=fukuda.html
8) D. Farkas, C. Du, G. Fisher, C. Lau, W. Niu, E. Wachman and R. Levenson: Comput. Med. Imag. Graphic. **22** (1998) 89.
9) R. Ornberg, B. Worner and D. Edwards: J. Histochem. Cytochem. **47** (1999) 1307.
10) R. Levenson and D. Farkas: Proc. SPIE **2983** (1997) 123.
11) C. Rothmann, Z. Malik and A. Cohen: Photoch. Photob. **68** (1998) 584.
12) C. Rothmann, A. Cohen and Z. Malik: J. Histochem. Cytochem. **45** (1997) 1097.
13) G. Siboni, C. Rothmann, B. Ehrenberg and Z. Malik: J. Histochem. Cytochem. **49** (2001) 147.
14) Z. Malik, C. Rothmann, T. Cycowitz and A. Ohen: J. Histochem. Cytochem. **46** (1998) 1113.
15) H. Fukuda, M. Yamaguchi, N. Ohyama and T. Wada: APIII, Pittsburgh, PA, 2002 http://apiii.upmc.edu/abstracts/posterarchive/2002/abs_include.cfm?file=fukuda_2.html
16) K. Fujii, M. Yamaguchi, N. Ohyama and K. Mukai: Proc. SPIE **4684** (2000) 1516.
17) A. Papadakis, E. Stathopoulos, G. Delides, K. Berberides, G. Nikiforidis and C. Balas: IEEE Trans. Biomed. Eng. **50** (2003) 207.
18) D. Haaland, R. Easterling and D. Vopicka: Appl. Spectrosc. **39** (1985) 73.
19) W. K. Pratt and C. E. Mancill: Appl. Opt. **15** (1976) 73.